Science and Technology Indonesia
e-ISSN:2580-4391 *p*-ISSN:2580-4405
Vol. 11, No. 1, January 2026

Research Paper

DPPH and Hep2 Cell Inhibitions by Ethyl Acetate Extract and Its Fractions from Indonesian *Cassia siamea* L. Stem Barks: In Vitro and Computational Prediction

Kartini Hasballah[1*], Murniana Murniana[2], Marlina Marlina [3], Bakhtiar Bakhtiar[4], Dewi Karlina Rusly[5], Binawati Ginting [2], Tika Maidiani[2], Shinta Rahmazani[2], Derren DCH Rampengan[6]

[1]*Department of Pharmacology, Faculty of Medicine, Universitas Syiah Kuala, Banda Aceh, 23111, Indonesia*
[2]*Department of Chemistry, Faculty of Mathematics and Natural Sciences, Universitas Syiah Kuala, Banda Aceh, 23111, Indonesia*
[3]*Department of Emergency Nursery, Faculty of Nursery, Universitas Syiah Kuala, Banda Aceh, 23111, Indonesia*
[4]*Department of Pediatrics, Faculty of Medicine, Dr. Zainoel Abidin General Hospital, Universitas Syiah Kuala, Banda Aceh, 23111, Indonesia*
[5]*Department of Obstetrics and Gynecology, Faculty of Medicine, Dr. Zainoel Abidin General Hospital, Universitas Syiah Kuala, Banda Aceh, 23111, Indonesia*
[6]*Faculty of Medicine, Universitas Sam Ratulangi, Manado, 95115, Indonesia*
***Corresponding author**: kartini.hasballah@usk.ac.id

Abstract
Cassia siamea has been reported by multiple ethnopharmacological studies to treat a broad spectrum of diseases, including cancer. The aim of this study was to evaluate the antioxidant and antiproliferation activities of *C. siamea* stem bark extract. Following the maceration, the sample was fractionated using column chromatography, yielding 1 ethyl acetate extract and 4 different fractions (Fractions A–D). Antioxidant activities of the extract and its four fractions were assessed based on the 2,2-diphenyl-1-picrylhydrazyl (DPPH) inhibition. Phytocompounds contained in the extract and its fractions were identified using Gas Chromatography-Mass Spectrometry (GC/MS) analysis, followed by in silico molecular docking. The ethyl acetate extract of *C. siamea* L. stem bark had total phenolic, flavonoid, and tannin contents of 280 mg GAE/g dry extract, 23.97 mg QE/g dry extract, and 26.5 mg TAE/ g dry extract, respectively. Strong antioxidant activities were exhibited by Fraction A and the ethyl acetate extract (IC_{50}= 13.72 and 14.10, respectively). LC_{50}s of the ethyl acetate extract and Fraction A against the *A. salina* larvae were 49.61 ppm and 51.52 ppm, respectively. Optimal inhibitions of Hep2 cell proliferation were observed in both ethyl acetate extract and Fraction A with IC_{50}s of 936.34 ppm and 580.76 ppm, respectively. Both the extract and Fraction A contained lupeol, among other compounds with anticancer potential. Complementary in silico docking analyses indicated that lupeol achieved optimal binding with laryngeal carcinoma–related targets (ΔG = –7.9 to 9.5 kcal/mol).

Keywords
Anticancer, Antioxidant, *Cassia sp.*, Ethnomedicine, Phytomedicine

Received: 12 August 2025, Accepted: 7 November 2025
https://doi.org/10.26554/sti.2026.11.1.235-251

1. INTRODUCTION

Comprehensive estimates on cancer prevalence and mortality worldwide by the International Agency for Research on Cancer reported that the cancer incidence almost reached 20 million in 2022 alone. The cancer-related mortality was reported to reach 9.7 million in 2022, with an estimated 1 in 9 men and 1 in 12 women dying from cancer (Bray et al., 2024). The trend of cancer prevalence, in general, is experiencing a significant increase (Chhikara and Parang, 2023). Such a concerning trend can be associated with the persistently growing pollution and unhealthy lifestyle problems (Iqhrammullah et al., 2023; Leiter et al., 2023; Qi et al., 2023). Thus, it is of importance to develop new strategies in cancer treatment, including the exploration of natural products with anticancer activities (Fikriah et al., 2024; Rahman et al., 2024). One of the approaches to explore such natural products is by screening plants that have been ethnomedicinally utilized in cancer treatment (Adedokun et al., 2024; Harahap et al., 2022; Tolo et al., 2023).

In this light, *Cassia siamea* Lamk. has been considered as an ethnomedicinal plant in many communities, where its traditional uses include the treatment of malaria, skin diseases, diabetes, inflammation, and wounds (Saising et al., 2022; Widiyastuti et al., 2024). The efficacy of *C. siamea* extract in various pathological conditions could be attributed to its rich contents of flavonoids and carotenoids (Kolar et al., 2018). In ethnomedicinal research, the roots of *C. siamea* are reported to be commonly used as anthelminthic and anticonvulsant (Ku-

mar et al., 2017; Olivier et al., 2024). In a previous study, the stem bark extract of *C. siamea* was found to contain an abundant amount of fatty acids such as 9,12-octadecadienoic acid (Z,Z) and n-hexadecanoic acid, which are attributable to the anti-inflammatory and antioxidant activities (Ogbiko, 2020). Another study found that the stem bark extract contained antioxidants such as caffeic acid and known anticancer agents such as cassanthraquinone A and 5-(hydroxymethyl)-2-methyl-6-prenylisoindolin-1-one (Adedokun et al., 2024). Phytocompound profiling in a Cassia plant (*Cassia mimosoides*) suggests high contents of alkaloids, flavonoids, and anthraquinone glycosides (Ezeabara et al., 2023).

Phytochemical profile of *C. siamea* determines the potency of its bioactivities, including that against cancer cells. Flavonoids inhibit the growth of cancer cells by scavenging free radicals, modulating oncologic signaling pathways, and regulating pro-/anti-apoptotic proteins (Kopustinskiene et al., 2020). The phenolic acids, such as caffeic acid could protect cells from DNA damage via its antioxidant activities, particularly because of its catechol moiety (Tatipamula and Kukavica, 2021). Moreover, phenolic acids can inhibit the proliferation of cancer cells by arresting the cell cycle at various phases (G1 or G2/M phases) (Kuruburu et al., 2022). As for the anthraquinones, the compounds are known to induce apoptosis in cancer cells by disrupting mitochondrial function and increasing reactive oxygen species production (Nowak-Perlak et al., 2023). The compounds were also reported to inhibit topoisomerase enzymes involved in DNA replication, leading to DNA damage and cancer cell death (Malik et al., 2021). The strong activities of anthraquinones in reducing cancer cell growth can be associated with the quinone structure in anthraquinones (Tian et al., 2020). The abundance of these compounds in *C. siamea* depends on the growing location. Previous studies reported the anticancer screening of *C. siamea* collected in Thailand and Africa (Gagman et al., 2020; Saising et al., 2022). Only a limited number of studies investigated *C. siamea* originating from Indonesia. A previous study reported the screening of *C. siamea* from three different locations in Indonesia. However, the previous study mainly focused on the antimalarial activity (Tasiam et al., 2020). The novelty of this study is the investigation of antioxidant and antiproliferation activities of *C. siamea* collected from Indonesia. The investigated extract was retrieved using ethyl acetate as a semipolar solvent, aiming at a wide range of bioactive compounds (Yusuf et al., 2023).

2. EXPERIMENTAL SECTION

2.1 Herbarium Specimen and Chemicals

Herbarium specimen was collected in October 2022 from the area around Kopelma Banda Aceh Regency, Aceh Province, Indonesia (5°34'06.6"N 95°21'53.3"E.). The specimen identification (B/518/UN11.1.8.4/TA.00.03/2023) at the Herbarium Laboratory of Universitas Syiah Kuala confirmed *C. siamea* L. Chemicals used in this study were DPPH, dimethyl sulfoxide (DMSO), silica gel, ethyl acetate, n-hexane, and methanol. Pharmaceutical-grade Vitamin C was purchased from PT. Supra Ferbindo Farma (Jawa Barat, Indonesia). Otherwise stated, all chemicals were analytical grade and purchased from Merck (Selangor, Malaysia).

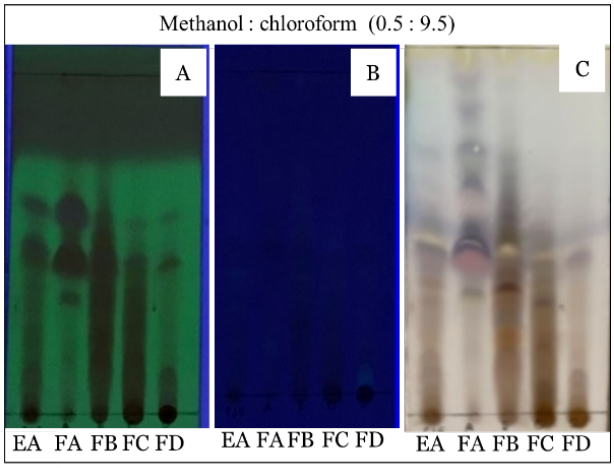

Figure 1. Thin-Layer Chromatography Chromatogram of Ethyl Acetate Extract from *C. siamea* L. Stem Bark and Its Fractions Eluted with Methanol : Chloroform (0.5 : 9.5) and Observed Under 254 nm UV Lamp (a), 366 nm UV Lamp (b), and with Vanillin Sulfate Reagent (c). EA, Ethyl Acetate Extract; FA, Fraction A; FB, Fraction B; FC, Fraction C; FD, Fraction D

2.2 Extraction and Fractionation of *Casssia siamea* L. Bark

As much as 10 kg of dried powder of *C. siamea* L. bark was macerated at room temperature using methanol solvent for four cycles (24 h/cycle). The filtrate was separated from the residue using a rotary evaporator (230 mbar; 10°C chiller; 55°C heating bath). The extract was then partitioned using n-hexane and ethyl acetate solvents to obtain the n-hexane and ethyl acetate extract sample. In a separating funnel, a mixture of n-hexane solvent and the previously obtained methanol extract was separated. The lipid residue was removed, whereas the soluble layer was collected and reconcentrated using a rotary evaporator under the same operating conditions.

Fractionation was further carried out on the ethyl acetate extract sample by means of gradient column chromatography (diameter = 5 cm and height = 50 cm). The ethyl acetate extract (7 g) was impregnated and inserted in a column containing preheated 150 g silica gel 60 GF_{254}, which was purchased from Merck (Selangor, Malaysia) with a specification of 230–240 mesh American standard testing and material (ASTM). The extract was firstly eluted with 100% n-hexane followed by n-hexane:ethyl acetate with 9:1, 8:2, and 7:3 ratios, sequentially. In total, 80 fractionation tubes were obtained, where each was subjected to thin-layer chromatography (TLC) analysis. Fractions having the same stain patterns were combined, resulting in only 4 fraction samples. The photographs of TLC patterns of each combined fraction obtained from

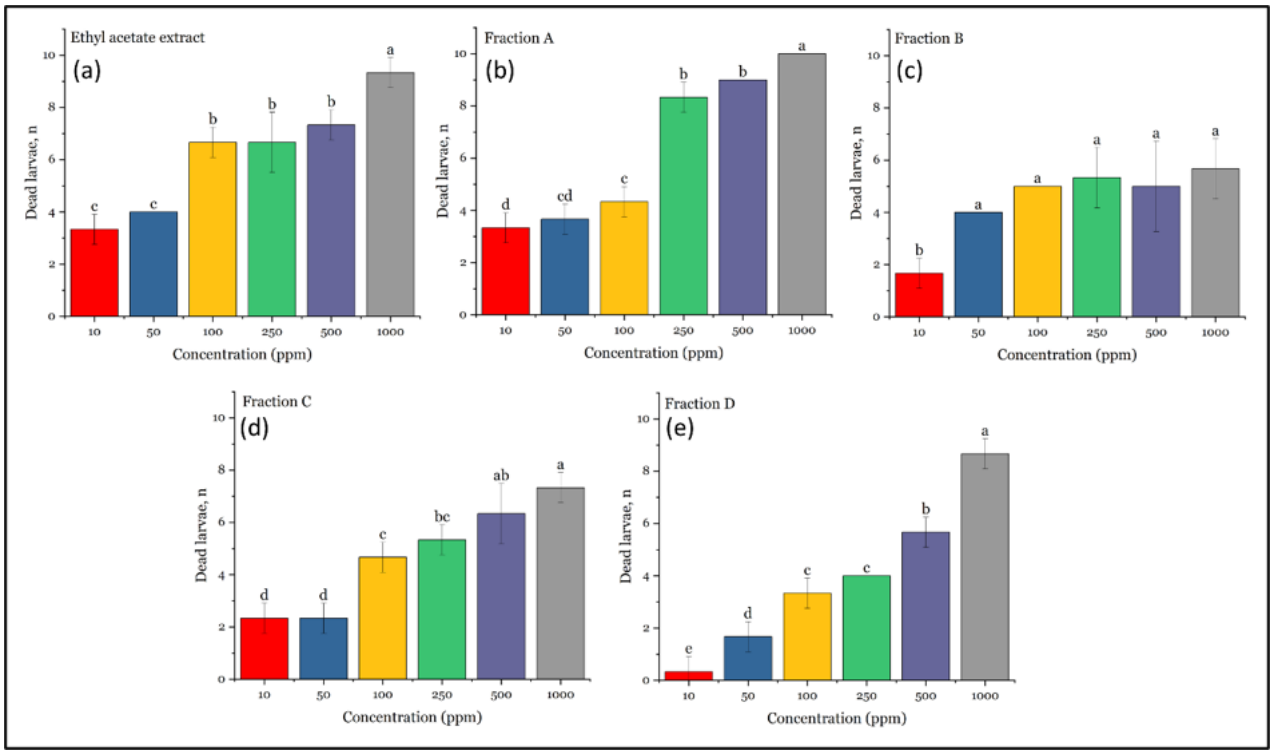

Figure 2. Effects of the Ethyl Acetate Extract from *Cassia siamea* L. Stem Bark (a) and Its Fractions, Including Fraction A (b), Fraction B (c), Fraction C (d), and Fraction D (e), on the Mortality of *A. salina* Larvae in Different Concentrations. Different Superscript Letters Denote Significant Differences ($p < 0.05$; Fisher's LSD).

the methanol:chloroform solvents of 0.5:9.5 are presented in Figure 1. All samples were subjected to phytochemical profiling using Gas Chromatography-Mass Spectrometry (GC/MS) analysis, with operating conditions matching those previously reported (Yusnaini et al., 2023).

2.3 Measurements of Total Phenolic, Flavonoid, and Tannin Contents

To measure the total phenolic content (TPC), the extract was prepared by dissolving it in 95% ethanol 95% (10 mg: 1 mL). As much as 100 μL was then added to a mixture containing 1 mL distilled water, 1.5 mL $NaHCO_3$ 2%, and Folin–Ciocalteu reagent (10% total mixture volume). Thereafter, the absorbance of the mixture was measured in a UV–vis spectrophotometer at 763 nm. The TPC was calculated based on the gallic acid calibration curve and expressed as mg gallic acid equivalent (GAE) /g dry extract.

As for the total flavonoid content (TFC) measurement, the *C. siamea* extract was initially dissolved in ethanol 95% (10 mg : 1 mL). Into the same reaction tube, 1 mL $AlCl_3$ 2% and 1 mL potassium acetate 120 nM were then added, followed by an hour of incubation. The absorbance was recorded at 435 nm in a UV–Vis spectrophotometer, where the TFC was expressed as mg quercetin equivalent (QE)/g dry extract.

To determine total tannic content (TTC), 0.5 g solid extract was initially dissolved in 10 mL distilled water, followed by the addition of Folin–Ciocalteu reagent (0.5 mL). After being left for 3 minutes, saturated Na_2CO_3 (1 mL) was then added to the mixture. Following the 15-minute incubation, the absorbance was measured at 740 nm in a UV–Vis spectrometer. The TTC was determined based on the tannic acid calibration curve ranged from 100 ppm to 300 ppm and expressed as mg tannic acid equivalent (TAE) /g dry extract.

2.4 2,2 Diphenyl 1 Picrylhydrazyl Assay

2,2-Diphenyl 1 picrylhydrazyl (DPPH) assay was performed with two repetitions following the procedure reported previously (Quranayati et al., 2023). Briefly, the respective samples (ethyl acetate extract and fractions A–D) were initially diluted in methanol to obtain 25, 50, and 100 ppm concentrations. The dissolved sample (5 mL) was inserted into a test tube and added with DPPH 0.4 mM (1 mL). The test tube was covered with aluminum foil and homogenized using a vortex mixer, then placed in an incubator for 30 minutes at 37°C. Inhibited DPPH free radicals were estimated using an ultraviolet-visible mini-1240 spectrophotometer (Kyoto, Japan) at λ =517 nm. With the same procedure, the antioxidant activity of ascorbic acid (3–9 ppm) was determined.

2.5 Brine Shrimp Lethality Test Assay

Before performing the brine shrimp lethality test (BSLT) assay, the *A. salina* eggs were hatched and grown for 48 h. Into each

Table 1. List of Ligand Candidates and Their Label (C1–23)

Ligand Candidate	Label
Butanamide, 2-hydroxy-N,2,3,3-tetramethyl-	C1
Benzaldehyde, 3-(chloroacetoxy)-4-methoxy-	C2
d-Mannose	C3
2-Propenoic acid, 3-(4-hydroxy-3-methoxyphenyl)-, methyl ester	C4
Hexadecanoic acid, methyl ester	C5
3-Amino-5-methoxyphenylpropionamide	C6
n-Hexadecanoic acid	C7
Dihydroartemisin, 6-deshydro-5-deshydroxy-3-desoxy-	C8
Methyl 3-(3,4-diethoxyphenyl)prop-2-enoate	C9
2,6-Dimethoxybenzaldehyde carbamoylhydrazone	C10
Dodecanoic acid, 2-hydroxy-1-(hydroxymethyl)ethyl ester	C11
10-Octadecenoic acid, methyl ester	C12
Methyl stearate	C13
3-Trifluoroacetoxypentadecane	C14
Azuleno[4,5-b]furan-2(3H)-one, decahydro-7,9-dihydroxy-6,9a-dimethyl-3-methylene-	C15
Octadecane, 3-ethyl-5-(2-ethylbutyl)-	C16
Bis(2-ethylhexyl) phthalate	C17
Octadecane, 3-ethyl-5-(2-ethylbutyl)-	C18
E-8-Methyl-9-tetradecen-1-ol acetate	C19
Lupeol	C20
Dimethyl dl-malate	C21
Hexadecanoic acid, methyl ester	C22
E-11-Hexadecenal	C23

test tube, saline water was added, followed by 10 previously hatched *A. salina* larvae. n-hexane extract and its fractions (FA–D) were dissolved in DMSO so that a variation of concentration of 1, 10, 100, 500, and 1000 ppm was obtained. Each concentration variation was added to the test tube containing *A. salina* larvae and stored under a tubular lamp. A test tube without the n-hexane extract or its fractions was taken as a control. After 24 h, the surviving and dead larvae were counted. This procedure was performed in two times repetition, where the number of dead larvae was averaged and presented as a mortality percentage. A linear curve equation was used to calculate the minimum concentration required to cause 50% mortality (LC_{50}).

2.6 3-(4,5-Dimethylthiazol-2-yl) -2-5 Diphenyl Tetrazolium Bromide (MTT) Assay

The Hep2 cell line, with an initial cell density of approximately $2.5–3.0 \times 10^4$ cells/well, was seeded into 96-well plates. Cells were incubated for 24 hours to allow for attachment and growth, after which they were washed with PBS. The cells were then treated with and without samples, specifically the Ethyl acetate extract from *C. siamea* L. bark and its five fractions (Fractions 1-5), each at a concentration of 1 mg/mL. For each sample, concentrations of 0.1, 0.3, 1, 3, 10, 30, and 100 μg/mL were prepared by dissolving the extract or fraction in DMSO, which was then added to the wells. Control wells received DMSO only. After a 72-hour incubation period, the medium was removed, and 10 μL of MTT solution (5 mg/mL in PBS, pH 7.2) was added to each well. Plates were incubated for an additional 4 hours at 37 °C. Following this incubation, 100 μL of DMSO (<0.5%) was added to each well, and the plate was shaken for 15 minutes to solubilize the formazan product. Subsequently, MTT-stop solution containing SDS was added, and the plates were incubated for another 24 hours. Absorbance was then measured at λ 540 nm using an ELISA reader to determine cell viability.

2.7 ADMET (Absorption, Distribution, Metabolism, Excretion, and Toxicity)

The metabolites identified by GC–MS from *C. siamea* ethyl acetate extract and Fraction A were subjected to in silico pharmacokinetic and toxicity screening. Twenty-three compounds were first selected on the basis of canonical SMILES availability in PubChem, labeled as C1-23 (Table 1). The SDF file was subsequently downloaded from PubChem. Canonical SMILES strings were submitted to the pkCSM platform and validated using the DeepPK server (Biosig Lab). The following parameters were predicted: Caco-2 permeability, human intestinal absorption (HIA), oral bioavailability probability (F20), plasma protein binding (PPB), volume of distribution at steady state (Vd), Ames mutagenicity, carcinogenicity, and maximum tolerated concentration (MTC). All results were extracted directly from the software outputs. Compounds predicted to have poor absorption or mutagenic potential were flagged for exclusion

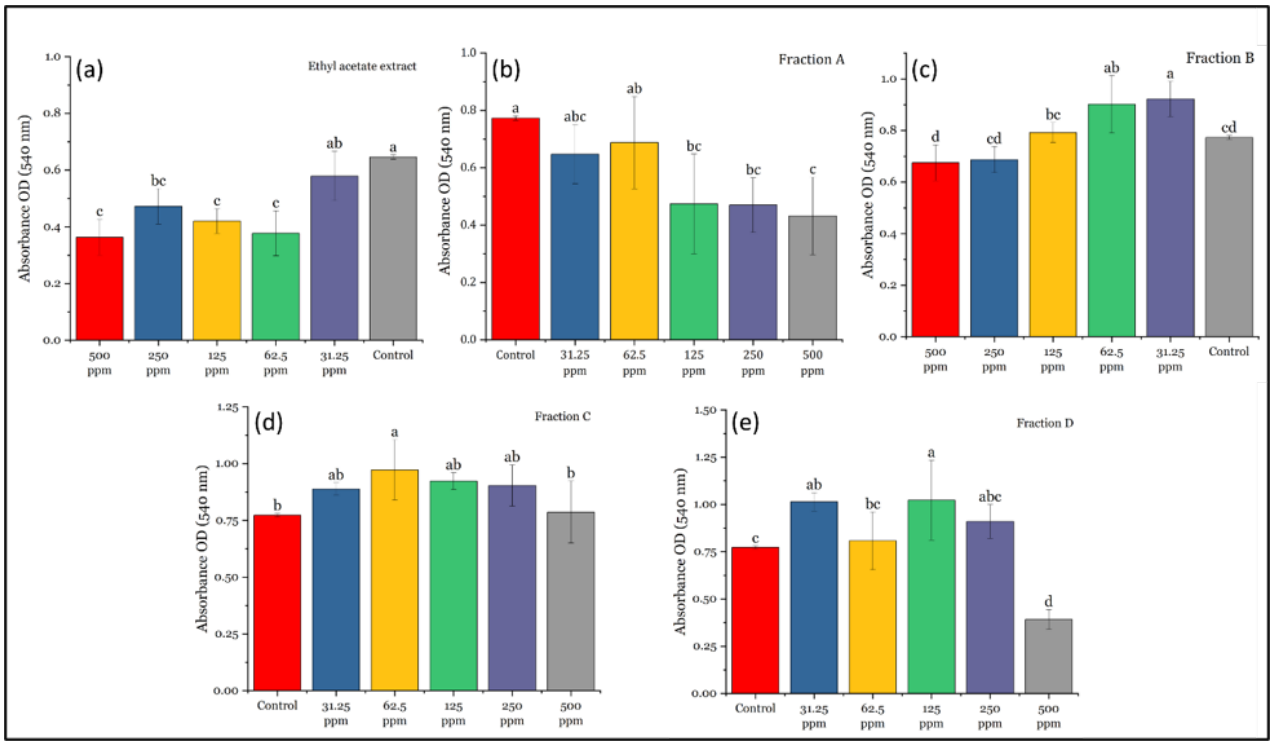

Figure 3. Effects of the Ethyl Acetate Extract from *Cassia siamea* L. Stem Bark (a) and Its Fractions, Including Fraction A (b), Fraction B (c), Fraction C (d), and Fraction D (e), on the Proliferation of Hep2 Cells in Different Concentrations. Different Superscript Letters Denote Significant Differences ($p < 0.05$; Fisher's LSD)

from subsequent analyses.

2.8 In Silico Molecular Docking and ADMET Prediction

The secondary metabolites identified from *C. siamea* stem bark were subjected to in silico screening to evaluate pharmacokinetic properties and molecular interactions with cancer-related targets, as recommended previously (Pomalango et al., 2025; Ramadhani et al., 2024). Twenty-three compounds (C1–23) were retrieved from PubChem in SDF format. ADMET properties, including were predicted using the pkCSM/DeepPK platforms.

Potential human protein targets for active compounds were predicted via SwissTargetPrediction using canonical SMILES input. Disease-related targets for laryngeal carcinoma were obtained from GeneCards and DisGeNET databases (relevance score > 5, gene–disease association ≥ 0.4). The overlap between predicted compound targets and laryngeal carcinoma-related genes was analyzed with Venny 2.1. STRING database (v12.0, Homo sapiens, confidence > 0.7) was used in the protein–protein interaction (PPI) networks construction, where the visualization was carried out using Cytoscape (v3.10.1). Enrichment analysis of Gene Ontology (GO) categories (Biological Process, Molecular Function, Cellular Component) and KEGG pathways was performed in DAVID with significance set at $p<0.05$ for the Benjamini–Hochberg parameters.

Molecular docking was performed using CBDock2 with blind docking mode against four key laryngeal carcinoma-related proteins: STAT3 (PDB: 6NUQ), AKT1 (PDB: 6HHF), EGFR (PDB: 8SC7), and HIF1A (PDB: 2ILM). Structures were retrieved from the Protein Data Bank. Ligands were docked as SDF files converted from PubChem. Protocol validation was carried out through re-docking of co-crystallized ligands, with root-mean-square deviation (RMSD) < 2.0Å considered acceptable. Binding affinities (ΔG, kcal·mol-1) and interaction residues were extracted, and docking complexes were visualized using Discovery Studio Visualizer (BIOVIA v24.1.0).

2.9 Data Analysis

Data distribution was analyzed using the Shapiro-Wilk test. Data with normal distribution were analyzed using one-way ANOVA with Fisher LSD post hoc test. Statistical significance was observed when $p<0.05$. The IC_{50} or LC_{50} is calculated based on the linear regression on probit values. In cases where the mortality reached 0% or 100%, Abbott's correction was applied. RStudio version 2024.04.2 was employed to perform the above-mentioned statistical computation.

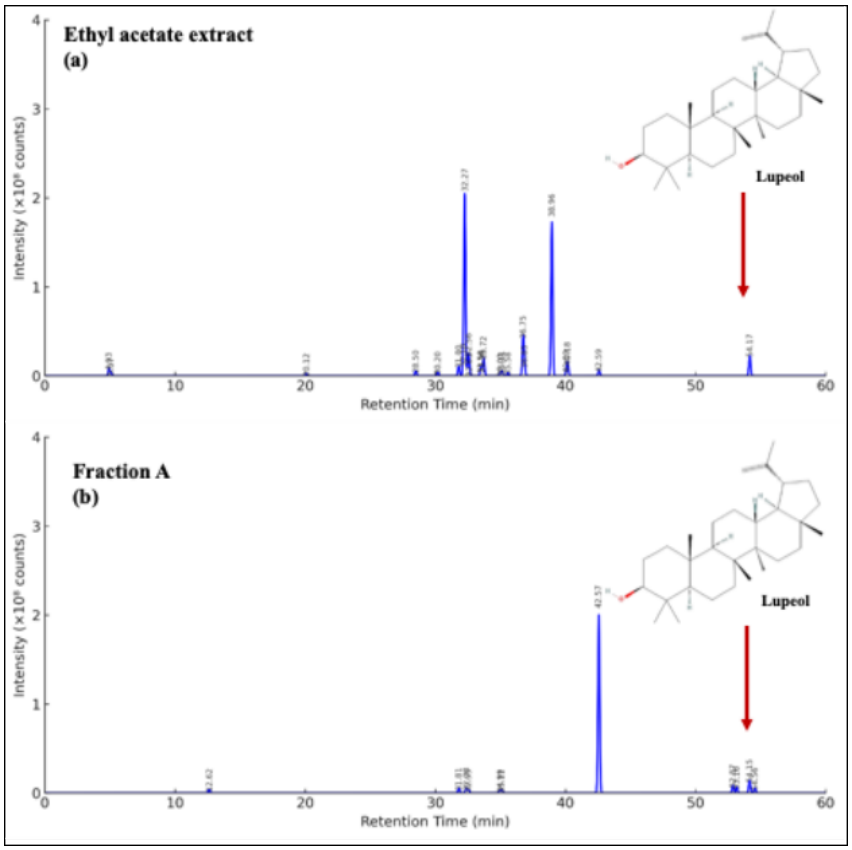

Figure 4. Chromatograms for Ethyl Acetate Extract of *C. siamea* Stem Barks (a) and Its Fraction A (b). Lupeol was Identified in Both Samples as Indicated by the Red Arrow

Table 2. Colors and Weights of the Ethyl Acetate Extract and Its Fractions from *Cassia siamea* L. Bark

Extract/Fraction	Container	Weight (g)	Color
Ethyl acetate extract	Not applicable	7.561	Green
Fraction 1	1-13	2.51	Dark green
Fraction 2	14-29	1.03	Brown
Fraction 3	30-60	0.39	Brown
Fraction 4	61-80	0.58	Brown

3. RESULTS AND DISCUSSION

3.1 Yield and Color Appearance of the Ethyl Acetate Extract and Its Fractions

We observed different colors of ethyl acetate extract and its fraction 1–4 from *C. siamea* L. bark. The extract weighed at 7.561 g with green color appearance. Fractions deriving from the extract had green as their base color, but varied in intensity. Chromatograms from the TLC analysis on the ethyl acetate extract and its fractions (Fraction A-D) are presented in Figure 1. A distinct separation for Fraction A and Fraction D was observed under the 254-nm UV lamp. Under a 366 nm UV lamp, minimal glowing was observed, indicating the presence of only a few fluorescent compounds. In the extract, several colored spots were visible, including brown and blue spots, accompanied by yellow and pink spots, which suggest the presence of multiple compounds. Fraction A displayed a small brown spot located near the baseline and a yellow spot at the top of the plate, indicating compounds that possibly include flavonoids or other pigments. Additionally, distinct pink, blue, and purple spots were observed, which could be indicative of phenolic compounds or anthocyanins. Fractions B and C are predominantly characterized by brown color, with smaller yellow spots in the middle. This suggests the presence of long-chain hydrocarbons or fatty acids. Fraction D exhibited a strong brown spot at the bottom, likely indicating a high concentration of a non-polar compound, and a faint purple spot in the middle, which may indicate the presence of anthocyanins or other flavonoid-related compounds. The summary of this observation is presented in Table 2.

3.2 In Vitro Antioxidant Capacities and Activities

The TPC and TFC of the extract were estimated to be 280 mg GAE/g dry extract and 23.97 mg QE/g dry extract, respectively. As for the TTC, the value reached 26.5 mg TAE/ g dry extract. The antioxidant activities were measured in vitro based on the DPPH assay, where the IC_{50}s for the ethyl acetate extract and its fractions are presented in Table 3. All

Table 3. Effectiveness of the Ethyl Acetate Extract from *C. siamea* L. Bark and Its Fractions According to DPPH, BSLT, and MTT (Hep2) Assays.

Sample	Equation	IC_{50}/LC_{50} (ppm)
DPPH assay		
Ethyl acetate extract	$y = 1.43x + 3.35$	14.10
Fraction A	$y = 1.06x + 3.79$	13.72
Fraction B	$y = 1.43x + 3.03$	23.70
Fraction C	$y = 1.73x + 2.39$	31.97
Fraction D	$y = 2.36x + 1.08$	46.31
Ascorbic acid	$y = 0.96x + 4.80$	1.60
BSLT assay		
Ethyl acetate extract	$y = 0.88x + 3.51$	49.61
Fraction A	$y = 1.10x + 3.11$	51.52
Fraction B	$y = 0.46x + 3.87$	275.57
Fraction C	$y = 1.11x + 2.34$	252.26
Fraction D	$y = 0.65x + 3.54$	175.32
MTT assay (Hep2)		
Ethyl acetate extract	$y = 0.60x + 3.21$	936.34
Fraction A	$y = 0.87x + 2.59$	580.76
Fraction B	$y = 0.26x + 3.16$	12.61×10^6
Fraction C	No inhibition	Not applicable
Fraction D	Inhibition only at 500 ppm	Not applicable

IC_{50} represents the concentration that inhibits 50% of the biological or biochemical activity. LC_{50} denotes the concentration that causes 50% mortality in the test population. All brine shrimps in the control (saline water) group survived.

samples had lower antioxidant capacity as compared to ascorbic acid (IC_{50}=1.6 ppm). The highest antioxidant capacity was achieved by Fraction A (IC_{50}=13.72 ppm), followed by the extract (IC_{50}= 14.10 ppm). As for Fractions B, C, and D, the IC_{50}s were 23.70 ppm, 31.97 ppm, and 46.31 ppm, respectively. At 100 ppm, the ethyl acetate extract, Fractions A–D, scavenged DPPH free radicals as much as 91.5%, 85.09%, 83.46%, 83.86%, and 83.31%, respectively.

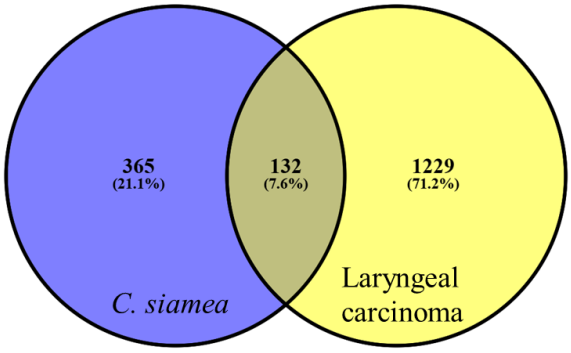

Figure 5. Venn Diagram Showing the Overlap Between Targets Identified from *C. siamea* and Genes/Targets Associated with Laryngeal Carcinoma

3.3 BSLT-Based Cytotoxicity

The effects of the *C. siamea* extract and its fractions on the mortality of *A. salina* larvae are presented in Figure 2. The effects are dose-dependent for all samples, except for Fraction B. The mortality of the larvae was significantly increased when by increasing the concentration was increased from 10 ppm to 50 ppm (p=0.014). However, no further changes in mortality were observed even when the concentration reached 1000 ppm. At the highest concentration (1000 ppm), the mortality reached 93.3%, 100%, 56.7%, 73.3%, and 86.7% when exposed to the ethyl acetate extract, Fractions A–D, respectively. The strongest cytotoxicity activity was yielded by the extract (LC_{50}=49.61 ppm), followed by Fraction A (LC_{50}=51.52 ppm). The LC_{50}s for all samples have been summarized and presented in Table 3.

3.4 Effectiveness against Hep2 Cell Proliferation

Results from the MTT assay against the Hep2 cell line are presented in Figure 3. In Fractions B and D, the inhibition was unlikely even at the highest concentration of 500 ppm. In Fraction D, the absorbance was even found to be significantly higher (p=0.022) when the concentration was set at 125 ppm. However, the inhibition was found to be significant (p<0.001) when the concentration was increased to 500 ppm. The effect of Fraction A exposure to the Hep2 cell culture was found to be dose-dependent, with the highest and significant inhibition observed at 500 ppm (p<0.001). The IC_{50}s of the extract

Table 4. Results for the Phytocompound Identification Using GC/MS

#	Identified compound	RT (min)	Area (%)	Sim. (%)
Ethyl acetate extract				
1	4-Methoxy-3-(trimethylsilyl)-1-octene	4.93	0.67	96
2	Butanamide, 2-hydroxy-N,2,3,3-tetramethyl-	5.07	0.43	98.6
3	Benzaldehyde, 3-(chloroacetoxy)-4-methoxy-	20.12	1.61	95
4	d-Mannose	28.5	0.44	97.5
5	2-Propenoic acid, 3-(4-hydroxy-3-methoxyphenyl)-, methyl ester	30.2	0.55	99.3
6	Hexadecanoic acid, methyl ester	31.8	2.63	95.9
7	Hexadecanoic acid, 3,5-bis(1,1-dimethylethyl)-4-hydroxy-, methyl ester	32.18	0.37	98.7
8	3-Amino-5-methoxyphenylpropionamide	32.27	1.45	98.9
9	n-Hexadecanoic acid	32.56	4.33	91.4
10	Dihydroartemisin, 6-deshydro-5-deshydroxy-3-desoxy-	33.5	0.47	98.4
11	Methyl 3-(3,4-diethoxyphenyl)prop-2-enoate	33.56	0.67	91.6
12	2,6-Dimethoxybenzaldehyde carbamoylhydrazone	33.72	2.09	96.8
13	Dodecanoic acid, 2-hydroxy-1-(hydroxymethyl)ethyl ester	35.01	1.37	98.5
14	10-Octadecenoic acid, methyl ester	35.11	1.68	100
15	Methyl stearate	35.58	2.62	94.7
16	3-Trifluoroacetoxypentadecane	36.75	0.68	90.2
17	3-Myristyl panthenate	36.85	0.56	98.2
18	3-(4-Methoxyphenyl)-(E)-2-Propenoic acid	38.96	0.88	90.8
19	Azuleno[4,5-b]furan-2(3H)-one,decahydro-7,9-dihydroxy-6,9a-dimethyl-3-methylene-	40.09	0.52	96.9
20	Octadecane, 3-ethyl-5-(2-ethylbutyl)-	40.18	0.59	100
21	Octadecane, 3-ethyl-5-(2-ethylbutyl)-1,2-ethanediol ester	41.76	0.4	100
22	Hexadecanoic acid, 1-(hydroxymethyl)-1,2-ethanediol ester	41.96	1.18	100
23	Bis(2-ethylhexyl) phthalate	42.59	65.09	100
24	Ethyl iso-alcoholate	43.21	0.48	100
25	Octadecane, 3-ethyl-5-(2-ethylbutyl)-	43.28	0.53	100
26	E-8-Methyl-9-tetradecen-1-ol acetate	44.73	0.61	91.2
27	Ergosta-5,22-dien-3-ol, acetate, (3$\hat{I}^2$,22E)-	49.03	0.44	94.8
28	Ethyl iso-alcoholate	49.91	0.47	98.9
29	W-18	50.8	0.38	99
30	W-18	53.01	0.37	98.3
31	Glycine, N-[(3a,5$\hat{I}^2$)-24-oxo-3-[(trimethylsilyloxy)cholan-24-yl]-methyl ester	53.27	0.5	95.1
32	W-18	53.48	0.4	99.4
33	Lupeol	54.17	1.13	97.6
34	W-18	55.74	0.49	99.5
Fraction A				
1	Dimethyl dl-malate	12.62	14.3	99.76
2	Hexadecanoic acid, methyl ester	31.81	2.57	94.3
3	1H-2-Benzopyran-1-one, 3,4-dihydro3,8- dihydroxy-3-methyl-, (-)-	32.38	7.53	99.53
4	1H-2-Benzopyran-1-one, 3,4-dihydro3,8- dihydroxy-3-methyl-, (-)-	32.55	2.4	99.63
5	Methyl 10-trans,12-cisoctadecadienoate	34.99	0.77	93.71
6	E-11-Hexadecenal	35.11	0.71	93.54
7	Bis(2-ethylhexyl) phthalate	42.57	65.58	99.89
8	(E)-4-Chloro-N-(1-(4-nitrophenethyl) piperidin-2-ylidene) benzene sulfonamide	52.87	0.3	99.52
9	Lupeol	54.15	4.32	98.4

RT: retention time

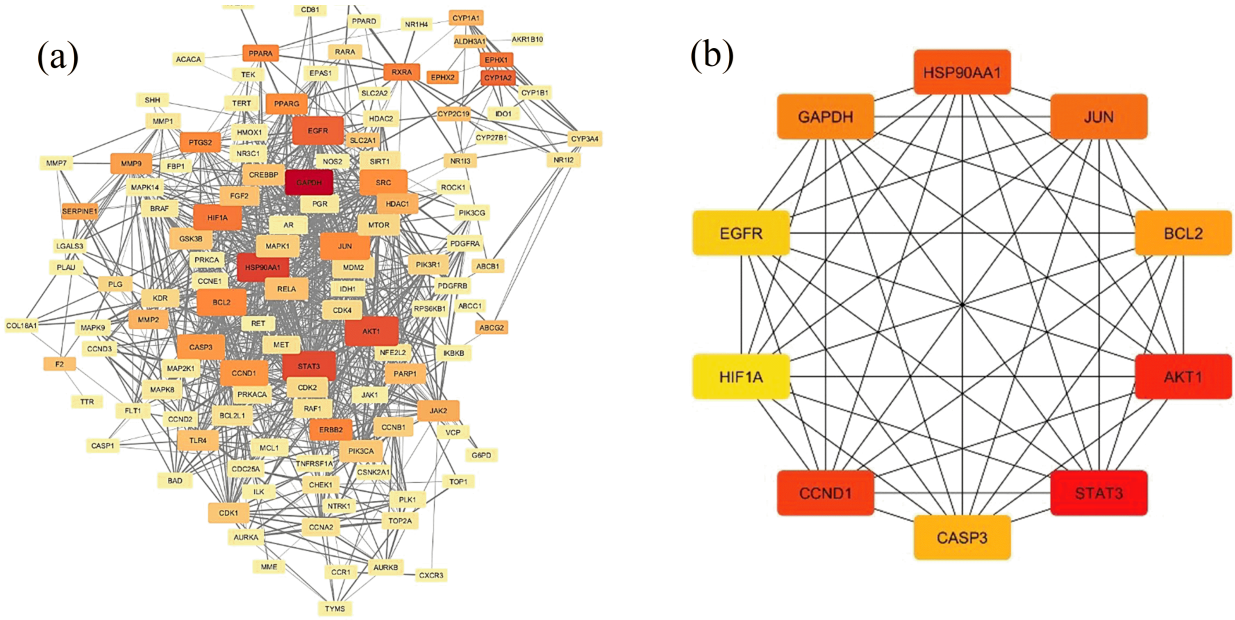

Figure 6. PPI Network of Overlapping *C. siamea*–Laryngeal Carcinoma Targets. Node color = Betweenness Centrality, Node Size = Degree, Edge Thickness = STRING Confidence Score. (b) Top 10 Hub Genes Ranked by MCC: GAPDH, HSP90AA1, JUN, BCL2, AKT1, STAT3, CASP3, CCND1, EGFR, HIF1A)

and its fractions for the MTT assay are presented in Table 3. The ethyl acetate extract and Fraction A reached the IC_{50}s of 936.34 ppm and 580.76 ppm, respectively. Fractions B and E had the IC_{50}s higher than 1000 ppm. The IC_{50}s for Fractions C and D could not be calculated because they showed no inhibition at the concentration range of 31.25 ppm to 500 ppm.

In this present study, the ethyl acetate extract of *C. siamea* stem barks was found containing rich phenolics, flavonoids, and tannins. The extract and its fraction were active in multiple assays, including DPPH assay, BSLT assay (*A. salina*), and MTT assay (Hep2). The extract and its Fraction A were found to be most active across the three assays. In comparison, lower antioxidant capacities were reported in a previous study investigating a wide range of Cassia species. The highest TPC and TFC were reported to be 200 GAE mg/g dry extract and 75 QE mg/g dry extract, respectively (Tomar and Srivastava, 2022). The antioxidant activities based on DPPH inhibition between those observed in the present study and previous studies are similar (Oyebade et al., 2021; Tasiam et al., 2020). Previously, the *C. siamea* aqueous extract had cytotoxic effect that was effective against *Caenorhabditis elegans* (Gagman et al., 2020). The cytotoxicity of this plant leaf extract has also been witnessed in human carcinoma cell lines with the IC_{50}s ranging from 135.81ppm to 235.52 ppm, depending on the cultivation location (Tasiam et al., 2020). The antioxidant activities of *C. siamea* extracts are consistently reported to be strong, while the cytotoxic effect was found to be potent across studies (Gagman et al., 2020; Oyebade et al., 2021; Tasiam et al., 2020; Tomar and Srivastava, 2022). Findings from this study regarding the efficacy of the extract against Hep2 cells significantly contribute to the significance of *C. siamea* as an alternative modality in cancer treatment and antioxidant therapies.

3.5 GC/MS Profiles of Ethyl Acetate Extract and Fraction A

Gas chromatography analysis was performed on ethyl acetate extract and Fraction A due to their high activity in across different assays in this study. The chromatograms for both samples are presented in Figure 4. More compounds were identified in the extract as compared to those of Fraction A. The extract contained methyl ferulate (0.55%) and dihydroartemisinin, 6-deshydro-5-deshydroxy-3-desoxy- (0.47%) (Table 4). As for Fraction A, the sample contained methyl 10-trans,12-cisoctadecadienoate (conjugated linoleic acid methyl ester) (0.77%). Lupeol, a compound with known anti-cancer potential, was found in both the extract and Fraction A. The concentration of lupeol is higher in Fraction A than in the extract (4.32% versus 1.13%).

In this present study, we have characterized the ethyl acetate extract of *C. siamea* stem bark and found that the extract is rich in phenolics, flavonoids, and tannins. The extract and its fraction were active in multiple assays, including the DPPH assay, BSLT assay (*A. salina*), and MTT assay (Hep2). The extract and its Fraction A were found to be most active across the three assays. In comparison, lower antioxidant capacities were reported in a previous study investigating a wide range of Cassia species. The highest TPC and TFC were reported to be 200 GAE mg/g dry extract and 75 QE mg/g dry extract,

Table 5. ADMET Screening Results for the *C. siamea* Secondary Metabolites (C1-23)

Compound	Caco-2	HIA	F20	PPB	Vd	Toxicity	Carcinogen	MTC
C1	-4.81	Absorbed	0.632	31.14	0.61	Safe	Safe	0.98
C2	-4.35	Absorbed	0.366	11.81	1.18	Safe	Safe	1.38
C3	-5.23	Absorbed	0.642	32.09	0.15	Safe	Safe	2.5
C4	-4.54	Absorbed	0.366	17.75	0.59	Safe	Safe	0.71
C5	-4.84	Absorbed	0.781	28.31	1.79	Safe	Safe	2.32
C6	-4.76	Absorbed	0.366	10.55	2.86	Safe	Safe	0.91
C7	-4.78	Absorbed	0.781	42.74	0.62	Safe	Safe	2.21
C8	-4.71	Absorbed	0.642	7.83	1.18	Safe	Safe	-0.35*
C9	-4.83	Absorbed	0.781	90.82	0.57	Safe	Safe	0.57
C10	-4.71	Absorbed	0.366	24.04	0.43	Safe	Safe	0.95
C11	-4.91	Absorbed	0.809	9.42	1.03	Toxic*	Safe	1.87
C12	-4.9	Absorbed	0.44	25.97	2.58	Safe	Safe	2.22
C13	-4.94	Absorbed	0.781	29.54	1.83	Safe	Safe	2.43
C14	-4.52	Absorbed	0.809	35.72	1.96	Toxic*	Safe	1.04
C15	-4.82	Absorbed	0.642	20.91	0.89	Safe	Safe	0.8
C16	-4.96	Absorbed	0.23*	17.31	3.71	Safe	Safe	1.41
C17	-4.58	Absorbed	0.642	41.39	3.32	Safe	Safe	0.96
C18	-4.96	Absorbed	0.23*	17.31	3.71	Safe	Safe	1.41
C19	-4.68	Absorbed	0.642	34.15	2.24	Safe	Safe	1.82
C20	-4.78	Absorbed	0.642	87.89	1.64	Safe	Safe	1.93
C21	-4.7	Absorbed	0.604	-7.54*	0.7	Safe	Safe	1.29
C22	-4.84	Absorbed	0.781	28.31	1.79	Safe	Safe	2.32
C23	-4.61	Absorbed	0.642	28.31	2.31	Safe	Safe	1.73

**Reason to exclude*

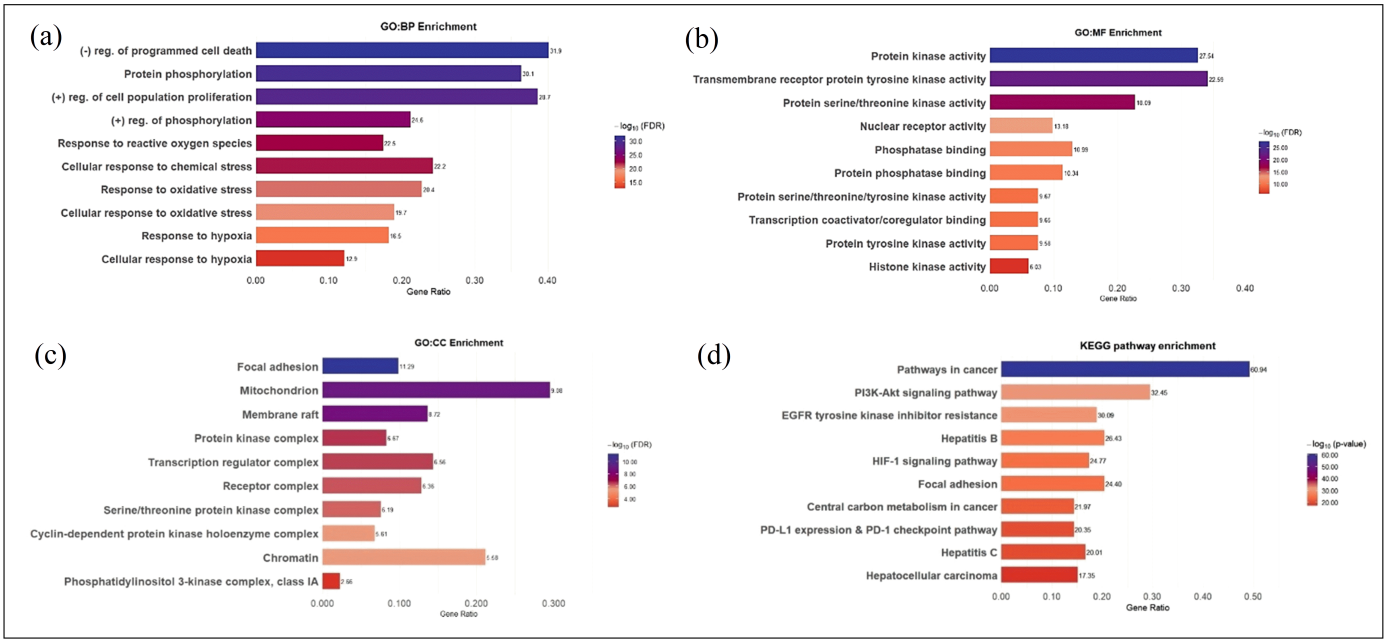

Figure 7. Gene Ontology (GO) and KEGG Enrichment Analysis of the 132 Overlapping *C. siamea*–Laryngeal Carcinoma Genes. (a) Top 10 GO Biological Processes, (b) Molecular Functions, (c) Cellular Components, and (d) KEGG Pathways

Table 6. Redocking Validation and Gridbox Parameters Used in Molecular Docking

Protein (PDB ID)	RMSD (Å)	Grid Size			Grid Position		
		X	Y	Z	X	Y	Z
STAT3 (6NUQ)	1.781	14	24	16	13.619	54.042	-0.083
AKT1 (6HHF)	0.8427	12	16	18	4.864	7.525	13.947
EGFR (8SC7)	1.277	18	10	12	21.68	0.772	50.704
HIF1A (2ILM)	1.860	10	6	8	19.675	25.596	28.272

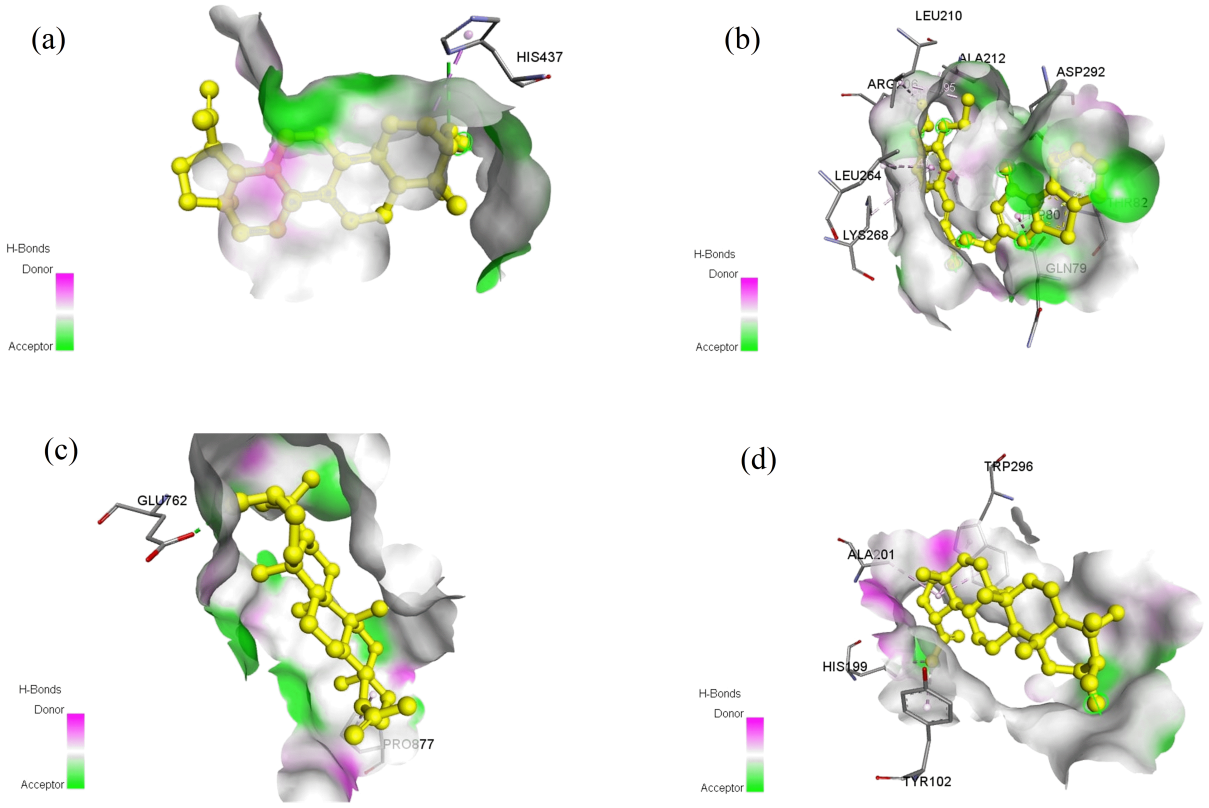

Figure 8. Three-Dimensional Illustration of the Molecular Binding Between Lupeol and the Pocket Regions of Roteins STAT3 (a), AKT1 (b), EGFR (c), and HIF1A (d)

respectively (Tomar and Srivastava, 2022). The antioxidant activities based on DPPH inhibition between those observed in the present study and previous studies are similar (Oyebade et al., 2021; Tasiam et al., 2020). Previously, the cytotoxic effect of aqueous extracts of *C. siamea* had been observed to be effective against *Caenorhabditis elegans* (Gagman et al., 2020). The cytotoxicity of this plant leaf extract has also been witnessed in human carcinoma cell lines, with the IC_{50}s ranging from 135.81ppm to 235.52 ppm, depending on the cultivation location (Tasiam et al., 2020). The antioxidant activities of *C. siamea* extracts are consistently reported to be strong, while the cytotoxic effect was found to be potent across studies (Gagman et al., 2020; Oyebade et al., 2021; Tasiam et al., 2020; Tomar and Srivastava, 2022). Findings from this study regarding the efficacy of the extract against Hep2 cells significantly contribute to the significance of *C. siamea* as an alternative modality in cancer treatment and antioxidant therapies.

Herein, the ethyl acetate extract was found to contain several bioactive compounds such as lupeol; 2-propenoic acid, 3-(4-hydroxy-3-methoxyphenyl)-, methyl ester (also known as methyl ferulate); dihydroartemisinin, 6-deshydro-5-deshydroxy-3-desoxy-; and benzenpropanoic acid, 3,5-bis(1,1-dimethylethyl)-4-hydroxy-, methyl ester. Lupeol is a triterpenoid that has demonstrated both antioxidant and anticancer activities, as suggested in multiple studies (Liu et al., 2021; Bhatt et al., 2021; Eldohaji et al., 2021; Malekinejad et al., 2022). In a meta-analysis of pre-clinical studies, lupeol was reported to be effective in reducing the tumor volume and weight in

Table 7. Binding Affinities of *C. siamea* Secondary Metabolites Toward Laryngeal Carcinoma-Related Proteins

Compounds	Binding Affinity (kcal · mol^{-1})			
	STAT	AKT	EGFR	HIF1A
C1	-4.7	-5	-4.7	-4.7
C2	-5.6	-6.7	-6.1	-6.2
C3	-4.9	-5.7	-5.8	-5.6
C4	-5.7	-5.6	-5.9	-6.2
C5	-4.5	-5.2	-6	-4.6
C6	-5.6	-6.6	-5.8	-5.9
C7	-4.6	-5.5	-5.5	-5.3
C9	-4.6	-10.2	-8.3	-7.9
C10	-6.3	-7.2	-5.8	-6.3
C12	-4.8	-6.6	-6	-5.2
C13	-4.8	-4.3	-6	-4.8
C15	-6.7	-8.3	-6.9	-7.2
C17	-5.3	-7.7	-6.6	-6.1
C19	-5.3	-7	-6.2	-5.4
C20*	-7.8	-9.5	-8.8	-7.9
C22	-4.5	-4.9	-5.6	-5.7
C23	-5	-6.3	-5.8	-5

*The highest binding score against all proteins.

different cancer models and administration routes (Fatma et al., 2024). Methyl ferulate is a derivative of ferulic acid, thus indicating the presence of this compound in the extract. Ferulic acid has strong antioxidant properties and the ability to inhibit tumor growth and promote cell apoptosis (Bao et al., 2023; Stompor-Gorący and Machaczka, 2021). Its antioxidant has been found useful in protecting the intestinal epithelial cells (Hwang et al., 2022). Antioxidant properties of ferulic acid can be attributed to the methoxyl on its benzene rings (Yang et al., 2021). Ferulic acid has a bioactivity to modulate cancer-related signaling pathways (Gupta et al., 2021; Herdiansyah et al., 2024; Singh Tuli et al., 2022). As for the dihydroartemisinin, 6-deshydro-5-deshydroxy-3-desoxy-, the compound is thought to be a derivative of artemisinin that has been reported in several studies to cause apoptosis in different types of cancer (Zeng et al., 2023). Benzenpropanoic acid, 3,5-bis(1,1-dimethylethyl)-4-hydroxy-, methyl ester has a similar structure with butylated hydroxytoluene (BHT) which is a synthetic antioxidant often used in food preservation (Sarmah et al., 2020). There are only limited studies reporting the protective effect of BHT against cancer cells (Ahmad et al., 2021; Fahim et al., 2023). Though limited, several studies suggest the toxicity of BHT that involves induced anxiety and reduced heart rate (Tortosa et al., 2020).

As for Fraction A, other than lupeol, the phytochemical analysis in the present study suggests the presence of coumarin derivative (1H-2-benzopyran-1-one, 3,4-dihydro3,8-dihydroxy-3-methyl-, [-]-), linoleic acid derivative (methyl 10-trans,12-cisoctadecadienoate), and palmitic acid derivative (hexadecanoic acid). Coumarins have been reported to effectively scavenge free radicals, with some of their derivatives exhibiting cytotoxic activities against cancer cells (Al-Warhi et al., 2020; Bhattarai et al., 2021). A recent report suggested that derivatives of coumarin and their structural hybrids can inhibit different isoforms of carbonic anhydrase enzymes, suggesting broad anticancer applications of these compounds (Rubab et al., 2022). Linoleic acid and its derivatives have been studied for their antiproliferative activities (Banni et al., 2020). Some studies have associated the antioxidant and anticancer activities of the investigated extract to the presence of linoleic acid (Al-Hwaiti et al., 2021; Morsi et al., 2020; Saffaryazdi et al., 2020).

3.6 ADMET Prediction of Identified Metabolites

In silico pharmacokinetic and toxicity screening was performed on 23 metabolites identified from the *C. siamea* ethyl acetate extract and Fraction A. The majority of compounds were predicted to be absorbed in the gastrointestinal tract and exhibited acceptable oral bioavailability probabilities (F20 range: 0.23–0.81). Most metabolites showed moderate to high predicted plasma protein binding and variable distribution volumes (0.15–3.71 L/kg). Two compounds (C11 and C14) were predicted as potentially mutagenic, while others were classified as non-mutagenic and non-carcinogenic. Predicted MTC values ranged from 0.57 to 2.50, suggesting tolerability within a reasonable range. These findings indicate that most metabolites from *C. siamea* demonstrate favorable ADMET properties, supporting their potential to exert biological effects. Compounds with unfavorable profiles (such as mutagenic predictions) were flagged for exclusion from further interpretation. Summarized

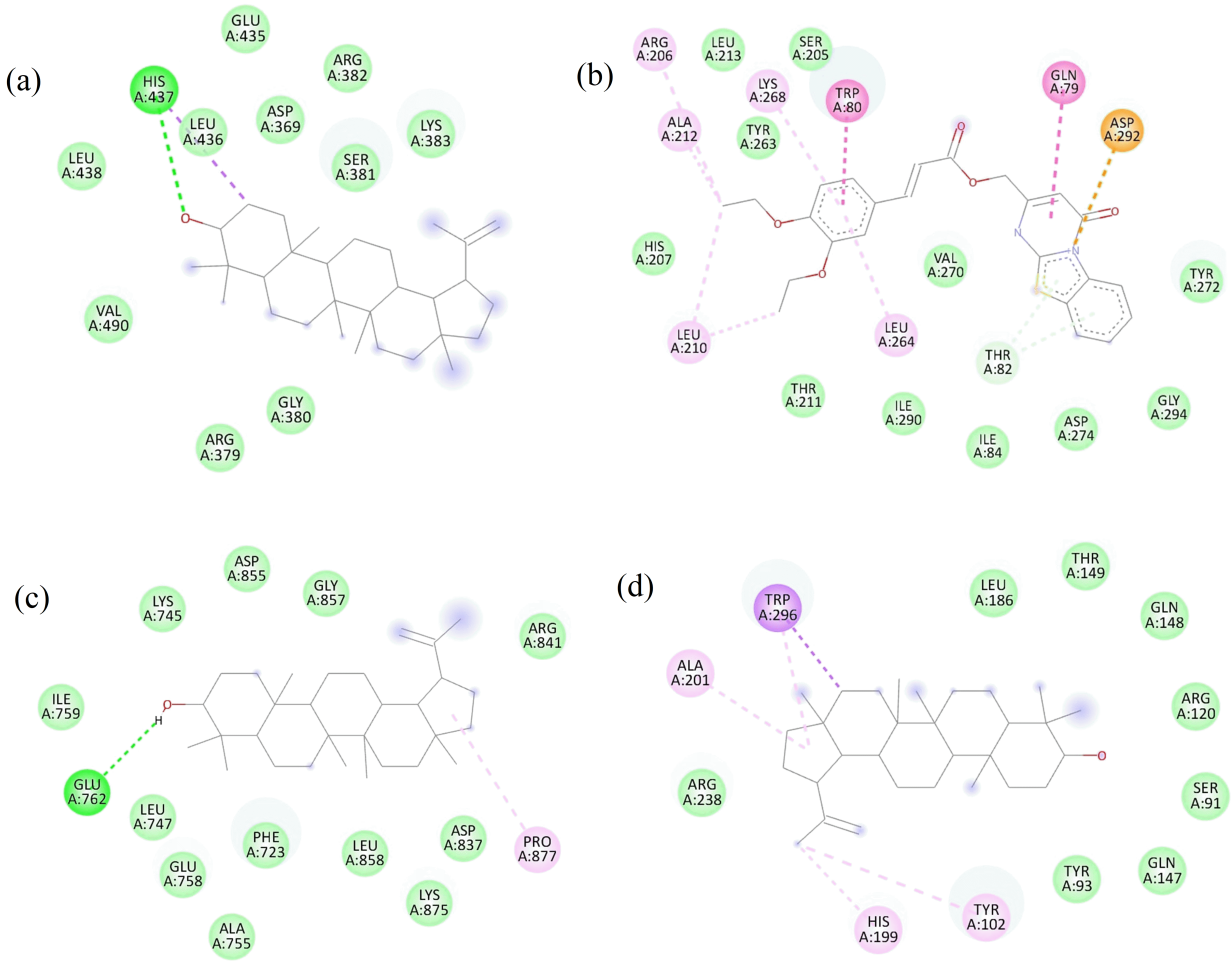

Figure 9. Three-Dimensional Illustration of the Molecular Bindings Between Lupeol and the Pocket Regions of Proteins STAT (a), AKT (b), EGFR (c), and HIF (d), Showing the Type of Interactions and Involved Residues

ADMET parameters of the ligand candidates is presented in Table 5.

3.7 Target Prediction and PPI Network Analysis

To identify potential protein targets of the metabolites, canonical SMILES of the 23 compounds were submitted to SwissTargetPrediction, and disease-related genes for laryngeal carcinoma were retrieved from GeneCards and DisGeNET. The overlap between compound-derived targets and laryngeal carcinoma–associated genes is presented in Figure 5. Out of the total predicted targets, 132 genes were found to be common to both datasets, representing candidates for further functional and docking analyses. The 132 overlapping targets between *C. siamea* metabolites and laryngeal carcinoma genes were further analyzed using the STRING database to explore their interaction profiles. The Cytoscape-derived PPI network visualization is presented in Figure 6a. In this network visualization, node color encodes betweenness-based centrality, node size scales with its degree (number of direct interactions), and edge thickness corresponds to the STRING combined confidence score. The network revealed several highly connected nodes, suggesting the presence of key regulators within the overlap set. To identify the most central genes, topological ranking was performed, yielding top 10 hub genes were GAPDH, HSP90AA1, JUN, BCL2, AKT1, STAT3, CASP3, CCND1, EGFR, as well as HIF1A (Figure 6b).

Functional enrichment analysis of the 132 overlapping targets revealed consistent patterns across GO and KEGG categories (Figure 7). The most significant biological processes were related to protein phosphorylation and kinase regulation, while molecular functions were dominated by protein kinase activity. Enrichment of cellular components highlighted membrane-associated structures such as receptor complexes and focal adhesions. KEGG pathway analysis indicated strong involvement of PI3K–AKT signaling, EGFR tyrosine kinase inhibitor resistance, focal adhesion, and HIF-1 signaling.

3.8 Molecular Docking Prediction

Herein, accuracy of the docking procedure was verified by re-docking native ligands into their respective active sites. The RMSD values ranged between 0.84 and 1.86 Å, all below the 2.0 Åthreshold, indicating that the docking protocol was sufficiently accurate for predicting ligand–protein interactions (Table 6). Binding affinity values varied across compounds and targets, with several metabolites showing predicted free energies of binding below –7.0 kcal·mol^{-1} (Table 7). Among these, Compound C20 displayed consistent affinities toward all four proteins, with values of –7.8 kcal·mol^{-1} (STAT3), –9.5 kcal·mol^{-1} (AKT1), –8.8 kcal·mol^{-1} (EGFR), and –7.9 kcal·mol^{-1} (HIF1A). Compound C9 (methyl 3-(3,4-diethoxyphenyl)prop-2-enoate) also showed a strong predicted affinity for AKT1 (–10.2 kcal ·mol^{-1}). Other compounds demonstrated moderate interactions, with scores ranging from –4.3 to –7.2 kcal·mol^{-1} depending on the target (Table 7). The three-dimensional illustration of the C20 (lupeol) binding to the pockets of STAT3, AKT1, EGFR, and HIF1A, showing the donor and acceptor region, is presented in Figure 8.

When interacting with STAT3, lupeol formed a stabilizing hydrogen bond with His437, supported by hydrophobic and polar contacts involving Leu436, Leu438, Val490, Arg379, Gly380, Ser381, Arg382, Lys383, Glu435, and Asp369, which collectively contributed to its stable binding orientation (ΔG = –7.8 kcal/mol) (Figure 9). In AKT1, lupeol was positioned within the conserved ATP-binding cleft between the N- and C-lobes of the kinase domain, engaging hinge-region residues Gln79 and Asp292 through key hydrogen bonds. These interactions were supplemented by polar contacts with Thr82, hydrophobic stabilization from Leu210, Ala212, Leu264, Val270, and Ile290, and π–π stacking with Trp80. Additional van der Waals contacts from Lys268, Tyr263, Arg206, and His207 reinforced the binding, producing the strongest predicted affinity (ΔG = –9.5 kcal·mol^{-1}). Within the lupeol-EGFR, a hydrogen bond with Glu762 anchored the ligand, while surrounding hydrophobic residues (Phe723, Leu747, Ile759, Ala755, Leu858) and polar interactions with Asp837, Arg841, and Pro877 stabilized the complex, yielding a high binding affinity (ΔG = –8.8 kcal·mol^{-1}). In lupeol-HIF1A complex, although no hydrogen bonds were detected, the small molecule was stabilized by extensive hydrophobic and aromatic contacts with Trp296, His199, Tyr102, Ala201, and Arg238, along with additional packing from Leu186, Gln148, Tyr93, and Arg120, resulting in an affinity comparable to STAT3 (ΔG = –7.9 kcal·mol^{-1}).

Findings of the present study are significant to the understanding of *C. siamea* therapeutic potential, particularly related to antioxidant therapies and anticancer treatment. However, several limitations in this research have to be acknowledged. First, the *C. siamea* was sampled from a single location; the concentrations of phytocompounds can be varied due to the differences in the growing environmental conditions. The interpretation of the antioxidant activity is also limited since the study only used a single in vitro assay. The MTT assay was also only performed in a single type of cell, and thus could not be extrapolated to different cells due to the differences in their physiology. Further, the identification was performed semi-quantitatively using the compound library for the reference. Studies in the future might consider carrying out the analysis on different in vitro assays and performing in-depth phytocompound profiling.

4. CONCLUSIONS

The ethyl acetate extract of *C. siamea* L. stem bark showed strong potential for antioxidant and anticancer applications. Fraction A demonstrated significant activity in scavenging DPPH free radicals and inhibiting the proliferation of the Hep2 cell line. GC/MS analysis identified several bioactive compounds, including lupeol, ferulic acid, coumarin, artemisinin, and hexadecenoic acid, which may contribute to these activities. To further support these findings, molecular docking was performed on representative compounds against laryngeal carcinoma–related targets. Among the tested molecules, lupeol exhibited the strongest predicted affinities, particularly for AKT1 and EGFR, followed by STAT3 and HIF1A. Detailed interaction analyses revealed that lupeol engaged hinge residues in the ATP-binding site of AKT1 and formed stable hydrogen bonds with STAT3 and EGFR, while hydrophobic and aromatic contacts dominated its interaction with HIF1A. These results suggest that compounds from *C. siamea* may act through multiple oncogenic signaling pathways, aligning with the observed antiproliferative activity in Hep2 cells. Further studies are warranted to validate these interactions experimentally and to explore their therapeutic relevance.

5. ACKNOWLEDGMENT

Authors appreciate the assistance from Universitas Syiah Kuala. This research was funded by Universitas Syiah Kuala and the Ministry of Education, Culture, Research, and Technology under contract number 141/UN11/SPK/PNBP/2022, dated 11 February 2022. The funders had no role in the study design, data collection and analysis, or interpretation of the results. The authors declare no known conflict of interest in relation to the publication of this work."

REFERENCES

Adedokun, O., M. Akinlo, I. Adedeji, O. Wande, O. Ume, N. Didacus, and O. Evans (2024). Unfolding the Cytotoxic Potential of *Cassia siamea* L.(Fabaceae) Stem via a Combination of Cost-Effective Anticancer Screening Templates. *Tropical Journal of Natural Product Research*, **8**(1); 6056–6061

Ahmad, M. H., W. A. Yehye, N. A. Rahman, L. A. Al-Ani, M. R. Johan, J. Lu, and N. M. Hashim (2021). Antioxidant and Cytotoxicity Activities of Butylated Hydroxytoluene Ligands Capped Gold Nanoparticles. *Chiang Mai J. Sci*, **48**(2); 405–419

Al-Hwaiti, M. S., E. M. Alsbou, G. Abu Sheikha, B. Bakchiche, T. H. Pham, R. H. Thomas, and S. K. Bardaweel (2021).

Evaluation of the Anticancer Activity and Fatty Acids Composition of "Handal" (*Citrullus colocynthis* L.) Seed Oil, a Desert Plant from South Jordan. *Food Science & Nutrition*, **9**(1); 282–289

Al-Warhi, T., A. Sabt, E. B. Elkaeed, and W. M. Eldehna (2020). Recent Advancements of Coumarin-Based Anticancer Agents: An Up-To-Date Review. *Bioorganic Chemistry*, **103**; 104163

Banni, S., S. D. Heys, and K. W. Wahle (2020). Conjugated Linoleic Acids As Anticancer Nutrients: Studies in Vivo and Cellular Mechanisms. In *Advances in Conjugated Linoleic Acid Research*. AOCS Publishing, pages 267–282

Bao, X., W. Li, R. Jia, D. Meng, H. Zhang, and L. Xia (2023). Molecular Mechanism of Ferulic Acid and Its Derivatives in Tumor Progression. *Pharmacological Reports*, **75**(4); 891–906

Bhatt, M., M. Patel, M. Adnan, and N. Reddy, M. (2021). Anti-Metastatic Effects of Lupeol Via the Inhibition of MAPK/ERK Pathway in Lung Cancer. *Anti-Cancer Agents in Medicinal Chemistry (Formerly Current Medicinal Chemistry-Anti-Cancer Agents)*, **21**(2); 201–206

Bhattarai, N., A. Kumbhar, A. R. Pokharel, Y. and N. Yadav, P. (2021). Anticancer Potential of Coumarin and Its Derivatives. *Mini Reviews in Medicinal Chemistry*, **21**(19); 2996–3029

Bray, F., M. Laversanne, H. Sung, J. Ferlay, L. Siegel, R. I. Soerjomataram, and A. Jemal (2024). Global Cancer Statistics 2022: GLOBOCAN Estimates of Incidence and Mortality Worldwide for 36 Cancers in 185 Countries. *CA: A Cancer Journal for Clinicians*, **74**(3); 229–263

Chhikara, B. and K. Parang (2023). Global Cancer Statistics 2022: The Trends Projection Analysis. Chemical Biology Letters. 2023

Eldohaji, M., L. B. Fayed, M. Hamoda, A. M. Ershaid, S. Abdin, B. Alhamidi, T. and S. Soliman, S. (2021). Potential Targeting of Hep3B Liver Cancer Cells by Lupeol Isolated from *Avicennia marina*. *Archiv der Pharmazie*, **354**(9); 2100120

Ezeabara, A., C. N. Umeka, L. and C. Anyanele, W. (2023). Phytochemical and Proximate Studies of Leaf, Stem and Root of *Cassia mimosoides* L. *International Journal of Scientific Research in Multidisciplinary Studies*, **9**(8); 38–45

Fahim, S. A., S. Ibrahim, S. A. Tadros, and O. A. Badary (2023). Protective Effects of Butylated Hydroxytoluene on the Initiation of N-Nitrosodiethylamine-Induced Hepatocellular Carcinoma in Albino Rats. *Human and Experimental Toxicology*, **42**; 09603271231165664

Fatma, H., M. Jameel, A. J. Siddiqui, M. Kuddus, N. S. Buali, I. Bahrini, and H. R. Siddique (2024). Chemotherapeutic Potential of Lupeol against Cancer in Pre-Clinical Model: A Systematic Review and Meta-Analysis. *Phytomedicine*, **132**; 155777

Fikriah, I., M. A. Masruhin, S. Paramita, E. Marliana, A. S. Panggabean, S. Ismail, and S. Y. Kim (2024). Acute Toxicity, Secondary Metabolites, and Antioxidant Activity of *Macaranga tanarius* from Post-Coal Mining and Non-Mining Areas in East Kalimantan, Indonesia. *Narra Journal*, **4**(2); e791

Gagman, H. A., N. A. I. I. N. Him, H. Ahmad, S. F. Sulaiman, R. Zakaria, and F. H. M. Termizi (2020). In Vitro Efficacy of Aqueous and Methanol Extract of *Cassia siamea* against the Motility of *Caenorhabditis elegans*. *Tropical Life Sciences Research*, **31**(3); 145–159

Gupta, A., A. K. Singh, M. Loka, A. K. Pandey, and A. Bishayee (2021). Ferulic Acid-Mediated Modulation of Apoptotic Signaling Pathways in Cancer. *Advances in Protein Chemistry and Structural Biology*, **125**; 215–257

Harahap, D., S. Niaci, V. Mardina, B. Zaura, I. Qanita, A. Purnama, and M. Iqhrammullah (2022). Antibacterial Activities of Seven Ethnomedicinal Plants from Family *Annonaceae*. *Journal of Advanced Pharmaceutical Technology & Research*, **13**(3); 148–153

Herdiansyah, M. A., R. Rizaldy, M. R. Alifiansyah, A. J. Fetty, D. Anggraini, N. Agustina, and H. S. Aulia (2024). Molecular Interaction Analysis of Ferulic Acid (4-Hydroxy-3-Methoxycinnamic Acid) As Main Bioactive Compound from Palm Oil Waste against MCF-7 Receptors: An in Silico Study. *Narra Journal*, **4**(2); e775

Hwang, H. J., S. R. Lee, J. G. Yoon, H. Moon, J. Zhang, E. Park, and J. A. Cho (2022). Ferulic Acid As a Protective Antioxidant of Human Intestinal Epithelial Cells. *Antioxidants*, **11**(8); 1448

Iqhrammullah, M., R. Y. Refin, R. I. Rasmi, F. F. Andika, H. Hajjah, M. Marlina, and R. Ningsih (2023). Cancer in Indonesia: A Bibliometric Surveillance. *Narra X*, **1**(2); e86

Kolar, F. R., C. L. Gogi, M. M. Khudavand, M. S. Choudhari, and S. B. Patil (2018). Phytochemical and Antioxidant Properties of Some *Cassia* Species. *Natural Product Research*, **32**(11); 1324–1328

Kopustinskiene, D. M., V. Jakstas, A. Savickas, and J. Bernatoniene (2020). Flavonoids As Anticancer Agents. *Nutrients*, **12**(2); 457

Kumar, D., A. Jain, and A. Verma (2017). Phytochemical and Pharmacological Investigation of *Cassia siamea* Lamk: An Insight. *The Natural Products Journal*, **7**(4); 255–266

Kuruburu, M. G., V. R. Bovilla, R. Naaz, Z. Leihang, and S. V. Madhunapantula (2022). Variations in the Anticancer Activity of Free and Bound Phenolics of Finger Millet (*Eleusine coracana* (l) Gaertn; Variety KMR-301) Seeds. *Phytomedicine Plus*, **2**(2); 100276

Leiter, A., R. R. Veluswamy, and J. P. Wisnivesky (2023). The Global Burden of Lung Cancer: Current Status and Future Trends. *Nature Reviews Clinical Oncology*, **20**(9); 624–639

Liu, K., X. Zhang, L. Xie, M. Deng, H. Chen, J. Song, J. Long, X. Li, and J. Luo (2021). Lupeol and Its Derivatives As Anticancer and Anti-Inflammatory Agents: Molecular Mechanisms and Therapeutic Efficacy. *Pharmacological Research*, **164**; 105373

Malekinejad, F., F. Kheradmand, M. H. Khadem-Ansari, and H. Malekinejad (2022). Lupeol Synergizes with Doxorubicin to Induce Anti-Proliferative and Apoptotic Effects on Breast

Cancer Cells. *DARU Journal of Pharmaceutical Sciences*, **30**(1); 103–115

Malik, M. S., R. I. Alsantali, R. S. Jassas, A. A. Alsimaree, R. Syed, M. A. Alsharif, and S. A. Ahmed (2021). Journey of Anthraquinones As Anticancer Agents - a Systematic Review of Recent Literature. *RSC Advances*, **11**(57); 35806–35827

Morsi, E. A., H. O. Ahmed, H. Abdel-Hady, M. El-Sayed, and M. A. Shemis (2020). GC-Analysis, and Antioxidant, Anti-Inflammatory, and Anticancer Activities of Some Extracts and Fractions of *Linum usitatissimum*. *Current Bioactive Compounds*, **16**(9); 1306–1318

Nowak-Perlak, M., P. Ziółkowski, and M. Woźniak (2023). A Promising Natural Anthraquinones Mediated by Photodynamic Therapy for Anti-Cancer Therapy. *Phytomedicine*, **119**; 155035

Ogbiko, C. (2020). Phytochemical, GC-MS Analysis and Antimicrobial Activity of the Methanol Stem Bark Extract of *Cassia siamea* (Fabaceae). *Asian Journal of Biotechnology*, **12**; 9–15

Olivier, B. M. B., D. L. Verlaine, F. Pistolesi, G. F. Houndjahoue, A. T. Guenefio, C. J. K. Nguinzanemou, and G. J. Chrysostome (2024). Traditional Herbal Medicine in the Central African Republic: Ethnobotanical Survey and Prognosis of Children Hospitalized at the Centre Hospitalier Universitaire. *Journal of Pediatrics & Neonatal Biology*, **9**(1); 1–14

Oyebade, K., A. Daspan, Y. Denkok, T. Alemika, and O. Ojerinde (2021). Antimicrobial, Antioxidant and Antiproliferative Properties of the Leaves of *Senna siamea*. *Journal of Complementary and Alternative Medical Research*, **14**(1); 22–29

Pomalango, Z. B., M. A. Paneo, N. Pakaya, L. O. Aman, and A. H. Hutuba (2025). Cholesterol-Lowering Effects of Turmeric Effervescent Dosage in Preventing Atherosclerosis. *Science and Technology Indonesia*, **10**(2); 482–492

Qi, J., M. Li, L. Wang, Y. Hu, W. Liu, Z. Long, and M. Zhou (2023). National and Subnational Trends in Cancer Burden in China, 2005–20: An Analysis of National Mortality Surveillance Data. *The Lancet Public Health*, **8**(12); e943–e955

Quranayati, Q., M. Iqhrammullah, N. Saidi, N. Nurliana, R. Idroes, and R. Nasution (2023). Extracts from *Phyllanthus emblica* L Stem Barks Ameliorate Blood Glucose Level and Pancreatic and Hepatic Injuries in Streptozotocin-Induced Diabetic Rats. *Arabian Journal of Chemistry*, **16**(9); 105082

Rahman, F. I., P. O. Zulfa, A. Beočanin, I. M. Faisal, N. Louca, M. I. Carstoiu, and H. Zufry (2024). Targeting Phosphoglycerate Dehydrogenase Enzyme Using Ginger Compounds to Suppress Thyroid Cancer Progression. *Narra X*, **2**(1); e112–e112

Ramadhani, F. A., M. F. Prastika, N. Fikriyah, Isnaeni, and N. W. Diyah (2024). Molecular Docking of Flavonoids from Extract of Roselle (*Hibiscus sabdariffa* L.) Calyx on PBP2a as the Basis for Antibacterial Activity Against Methicillin Resistant *Staphylococcus aureus*. *Science and Technology Indonesia*, **9**(2); 487–493

Rubab, L., S. Afroz, S. Ahmad, S. Hussain, I. Nawaz, A. Irfan, and M. Mojzych (2022). An Update on Synthesis of Coumarin Sulfonamides as Enzyme Inhibitors and Anticancer Agents. *Molecules*, **27**(5); 1604

Saffaryazdi, A., A. Ganjeali, R. Farhoosh, and M. Cheniany (2020). Variation in Phenolic Compounds, α-Linolenic Acid and Linoleic Acid Contents and Antioxidant Activity of Purslane (*Portulaca oleracea* L.) during Phenological Growth Stages. *Physiology and Molecular Biology of Plants*, **26**; 1519–1529

Saising, J., K. Maneenoon, O. Sakulkeo, S. Limsuwan, F. Götz, and S. P. Voravuthikunchai (2022). Ethnomedicinal Plants in Herbal Remedies Used for Treatment of Skin Diseases by Traditional Healers in Songkhla Province, Thailand. *Plants*, **11**(7); 880

Sarmah, R., S. Kanta Bhagabati, R. Dutta, D. Nath, H. Pokhrel, L. P. Mudoi, and R. Jyoti Nath (2020). Toxicity of a Synthetic Phenolic Antioxidant, Butyl Hydroxytoluene (BHT), in Vertebrate Model Zebrafish Embryo (*Danio rerio*). *Aquaculture Research*, **51**(9); 3839–3846

Singh Tuli, H., A. Kumar, S. Ramniwas, R. Coudhary, D. Aggarwal, M. Kumar, and K. Sak (2022). Ferulic Acid: A Natural Phenol That Inhibits Neoplastic Events through Modulation of Oncogenic Signaling. *Molecules*, **27**(21); 7653

Stompor-Gorący, M. and M. Machaczka (2021). Recent Advances in Biological Activity, New Formulations and Prodrugs of Ferulic Acid. *International Journal of Molecular Sciences*, **22**(23); 12889

Tasiam, E., R. Primaharinastiti, and W. Ekasari (2020). In Vitro Antimalarial Activity and Toxicity Studies of Johar (*Cassia siamea*) Leaves from Three Different Locations. *African Journal of Infectious Diseases*, **14**(2); 23–29

Tatipamula, V. B. and B. Kukavica (2021). Phenolic Compounds As Antidiabetic, Anti-Inflammatory, and Anticancer Agents and Improvement of Their Bioavailability by Liposomes. *Cell Biochemistry and Function*, **39**(8); 926–944

Tian, W., C. Wang, D. Li, and H. Hou (2020). Novel Anthraquinone Compounds As Anticancer Agents and Their Potential Mechanism. *Future Medicinal Chemistry*, **12**(7); 627–644

Tolo, C. U., I. Kahwa, U. Nuwagira, A. Weisheit, and H. Ikiriza (2023). Medicinal Plants Used in Treatment of Various Diseases in the Rwenzori Region, Western Uganda. *Ethnobotany Research and Applications*, **25**; 1–16

Tomar, V. and M. Srivastava (2022). Comparative Phytochemical Estimation and Free Radical Scavenging Activity in Leaves of *Cassia* Species. *National Academy Science Letters*, **45**(3); 227–229

Tortosa, V., V. Pietropaolo, V. Brandi, G. Macari, A. Pasquadibisceglie, and F. Polticelli (2020). Computational Methods for the Identification of Molecular Targets of Toxic Food Additives. Butylated Hydroxytoluene As a Case Study. *Molecules*, **25**(9); 2229

Widiyastuti, Y., D. Subositi, S. Haryanti, R. Mujahid, and

U. Siswanto (2024). Exploration and Characterization of Johar (*Cassia siamea*) Accession as a Source of Raw Material for Antimalaria Drug. In *IOP Conference Series: Earth and Environmental Science*, volume 1362. IOP Publishing, page 012039

Yang, J., J. Chen, Y. Hao, and Y. Liu (2021). Identification of the DPPH Radical Scavenging Reaction Adducts of Ferulic Acid and Sinapic Acid and Their Structure-Antioxidant Activity Relationship. *Lwt*, **146**; 111411

Yusnaini, R., R. Nasution, N. Saidi, T. Arabia, R. Idroes, I. Ikhsan, R. Bahtiar, and M. Iqhrammullah (2023). Ethanolic Extract from *Limonia acidissima* L. Fruit Attenuates Serum Uric Acid Level Via URAT1 in Potassium Oxonate-Induced Hyperuricemic Rats. *Pharmaceuticals*, **16**(3); 419

Yusuf, H., H. Novia, and M. Fahriani (2023). Cytotoxic Activity of Ethyl Acetate Extract of *Chromolaena odorata* on MCF7 and T47D Breast Cancer Cells. *Narra J*, **3**(3); e326

Zeng, Z.-w., D. Chen, L. Chen, B. He, and Y. Li (2023). A Comprehensive Overview of Artemisinin and Its Derivatives As Anticancer Agents. *European Journal of Medicinal Chemistry*, **247**; 115000

